**Steel and Composite Structures**, *Vol. 23, No. 2 (2017) 217-228*
DOI: https://doi.org/10.12989/scs.2017.23.2.217


# Local and global buckling condition of all-steel buckling restrained braces

Seyed Masoud Mirtaheri [*1], Meissam Nazeryan [2a], Mohammad Kazem Bahrani [3b], Amin Nooralizadeh [3c], Leila Montazerian [4d] and Mohamadhosein Naserifard [5e]

[1] *Department of Civil Engineering, K.N. Toosi University of Technology, Tehran, Iran*
[2] *Department of Civil Engineering, Sharif University of Technology, Tehran, Iran*
[3] *Department of Civil Engineering, University of Qom, Qom, Iran*
[4] *Department of Civil Engineering, Chalus Branch, Islamic Azad University, Chalus, Iran*
[5] *Department of Civil Engineering, Yazd Branch, Islamic Azad University, Yazd, Iran*

(*Received May 23, 2016, Revised December 10, 2016, Accepted December 22, 2016*)

**Abstract.** Braces are one of the retrofitting systems of structure under earthquake loading. Buckling restrained braces (BRBs) are one of the very efficient braces for lateral loads. One of the key needs for a desirable and acceptable behavior of buckling-restraining brace members under intensive loading is that it prevents total buckling until the bracing member tolerates enough plastic deformation and ductility. This paper presents the results of a set of analysis by finite element method on buckling restrained braces in which the filler materials within the restraining member have been removed. These braces contain core as the conventional BRBs, but they have a different buckling restrained system. The purpose of this analysis is conducting a parametric study on various empty spaces between core and restraining member, the effect of friction between core and restraining member and applying initial deformation to brace system to investigate the global buckling behavior of these braces. The results of analysis indicate that the flexural stiffness of restraining member, regardless of the amount of empty space, can influence the global buckling behavior of brace significantly.

**Keywords:** buckling restrained brace (BRB); finite element method; cyclic loading; global buckling

## 1. Introduction

Buckling restrained brace (BRB) is a kind of new seismic restraining system which is being widely used due to its efficiency and better seismic performance than conventionall brace. BRBs are usually used in centeric braced frames. In common structures which have been retrofitted against earthquake by steel braces, the major loss of energy happens when braces are under tension and they lose a great deal of energy through yielding but under pressure, they buckle before reaching to yield stress and the energy dissipation of the BRB decreases thus the stability of structures will be endangered due to unstable brittle buckling. It can be said that BRBs are a kind of CBF in which the brace buckling under compression has been prevented. In these braces, the hysteretic performance of brace is similar to that of core materials. BRBs' basic performance principle is that under pressure, resistance against stress is separated from resistance against flexural buckling. From other properties of these braces is that the ductility of steel materials takes place in a considerable length of the brace. As shown in Fig. 1, a typical BRB consists of a steel core, buckling restraining mechanism (BRM) and a separating space(gap) between BRM and steel core for independent axial deformation of internal core . At first, the buckling restraininig member was a steel section filled with concrete, which forms a member with high rigidity but in total steel braces which are considered as the new generation of these braces, the buckling restrained member is completely composed of steel. In a conventional all- steel brace, the inner steel core has been restrained through a buckling -restraining system made up of steel members; which in this system there is no more need to concrete materials that were once common in BRBs and therefore, concrete materials are removed from this system and as a result, the time of construction and cost will decrease. Moreover, this system can be investigated easily after earthquake.

Component testing of BRBs were performed by Black *et al*. (2002) and the results showed that unbonded brace is an appropriate alternative to conventional lateral load-resisting systems, and is able to increase the earthquake resistance of new and existing structures. Sabelli *et al*. (2003) focused on the seismic behavior of buckling-restrained braces in the case of use in concen-trically braced frames, and Fahnestock *et al*. (2007) conducted a numerical and large-scale experimental program to study the seismic response of BRBs using a nonlinear dynamic analysis. A seismic design process for BRBF based on energy waste and a direct displacement design process was provided (Kim and Choi 2004, ATC 1996). A test program on six all-steel buckling

*Corresponding author, Ph.D., Associate Professor, E-mail: mmirtaheri@kntu.ac.ir
[a] M.Sc., E-mail: Meissamnazeryan@gmail.com
[b] Assistant Professor, E-mail: M.bahrani@iiees.ac.ir
[c] Ph.D. Student, E-mail: Aminnooralizadeh@stu.nit.ac.ir
[d] M.Sc., E-mail: Lmontazeri88@gmail.com
[e] M.Sc., E-mail: Naserimail@yahoo.com


http://www.techno-press.org/?journal=scs&subpage=6
ISSN: 1229-9367 (Print), 1598-6233 (Online)

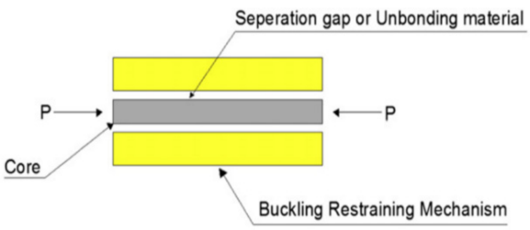


Fig. 1 Members of BRB (Tremblay *et al.* 2006)

-restrained braces (BRBs) and also a test on a conventional bracing member for comparison purposes was performed by Tremblay *et al.* (2006). An experimental study on the hysteretic response of all-steel BRBs with different cross sections and details was also conducted by Eryasar (2009). Takeuchi *et al.* (2012) studied the Effect of local buckling core plate restraint in buckling restrained braces under cyclic loading tests on BRBs with various mortar restrainers and circular tube thicknesses. Cyclic test of buckling restrained braces composed of square steel rods and steel tube were carried out on six buckling-restrained braces (BRBs) with a gap between the core and the tube filled with steel rods as filler material by Park *et al.* (2012). The test results showed satisfactory performance of the BRB with continuous steel rods as filler material but not for discontinuous steel rods. Eight BRB specimens with various core width-to-thickness ratios and the gap between the core and the casing were tested by Zhao *et al.* (2014) to investigate the Local buckling behavior of steel angle core members in buckling-restrained braces. The results showed two types of local buckling modes of the core and no local failure of the casing impelled by local buckling was observed. Chen *et al.* (2016) conducted experimental tests on seven all-steel buckling-restrained braces (BRBs) with a layer of 1-mm thick gap between the core and the restraining system to investigate the effect of the unbonding materials. Test results indicated the deformations sustainability of all the BRBs. Jiang *et al.* (2015) studied the overall performance of buckling-restrained braces through refined finite element (FE) model via considering the contact interaction between the core and external restraining members that led to propose the recommended values of core width-to-thickness ratio, core thickness. Talebi *et al.* (2015) studied the effects of size and type of filler material through a three-dimensional numerical analysis on the performance of buckling restrained braces at fire. The study showed the premier fire performance of BRB with metal filler material in the gap than concrete as well as by increasing the size of the gap. Kim and Choi (2015) suggested reinforcing H-shaped braces with non-welded cold-formed stiffeners to restrain flexure and buckling through a finite element analysis. Wu and Mei (2015) studied the buckling mechanism of the steel core of buckling-restrained braces. The results indicate that increasing axial load affects the development of buckling mode. Also the results led to obtaining the formulae of the maximum contact force and the maximum bending moment of the restraining member. Experimental tests were carried out on the reduced-core length BRB (RCLBRB) specimens including detachable casings to investigate the influence of variable core clearance and the local detailing of casings on the cyclic performance of RCLBRB specimens. The results showed the strain sustainability up to a core strain of 4.2% and nearly the same strength-adjustment factors for the RCLBRB specimens and conventional BRBs as noticed in the past studies (Pandikkadavath and Sahoo 2016).

## 2. Derivation of overall buckling prevention conditional equation

At present, the most common conditional expression used in relation to buckling prevention of BRBs which are placed on the simple supports at both ends, is defined as (JSSC 1998)

$$\frac{P_{\max}\left(a+d+e\right)}{1-\dfrac{P_{\max}}{P_E^R}} \leq M_y^R \tag{1}$$

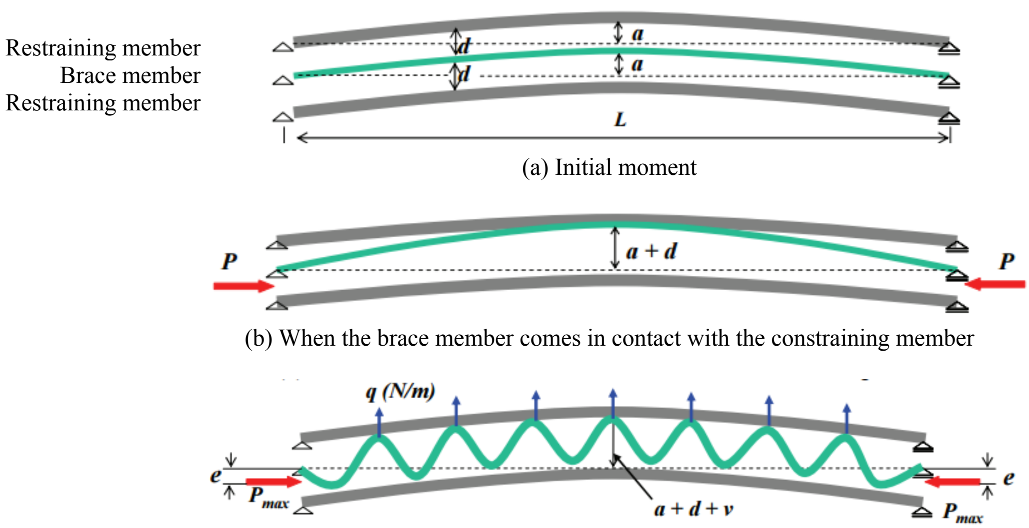


(a) Initial moment

(b) When the brace member comes in contact with the constraining member

(c) Immediately after global buckling

Fig. 2 Behavior of BRB up to occurrence of global buckling (Usami *et al.* 2009)

In this relation $M_y^R$: equals yield moment of bulking restraining member, $P_{max}$: The maximum axial compression force acting on bracing member, $P_E^R$: Euler buckling load of bulking restraining member, $a$: initial deformation at the center of the restraining member, $d$: the distance between bracing member and bulking resisting member, $e$: eccentricity of axial compression force (equal at both ends).

The left side of this inequality is the required bending moment at the center of buckling restraining member in which the effects of $P$-$\Delta$ are taken into account, and the right side of the inequality is the yield bending strength (capacity) of buckling restraining member, in addition this inequality shows that the initial yielding has been assumed as limit state. The derivation of the above inequality is shown in Fig. 2.

Based on the results obtained from the research conducted by Kato *et al*. (2002) the derivation of the above equation is shown below. The bending moment formed at the center of BRBs, is obtained as follows after occurrence of overall buckling

$$M_c = P_{max}\left(a+d+e+v\right) \quad (2)$$

Where in this relation ν is the lateral deformation of restraining member after global buckling and $M_c$ is the bending moment, generated at the center of BRB after the occurrence of overall buckling.

$$v = \frac{5M_c L^2}{48E^R I^R} \quad (3)$$

According Eqs. (3) and (2), at the moment of global buckling, it is assumed that

$$M_c = \frac{P_{max}\left(a+d+e\right)}{1-\dfrac{5P_{max}L^2}{48E^R I^R}} \cong \frac{P_{max}\left(a+d+e\right)}{1-1.03\dfrac{P_{max}}{P_E^R}} \quad (4)$$

In which $P_E^R$ is the Euler buckling load of the restraining member is

$$P_E^R = \frac{\pi^2 E^R I^R}{L^2} \quad (5)$$

Where $E$ is the elastic modulus, $L$ is the length of the brace, and $I$ is the second moment of inertia of the external tube.

Therefore, assuming that $P_{max} = P_y$ in Eq. (4) it is clear that in this relation the ratio of $P_e/P_y$ will be very effective in determination of bending moment.

Chen *et al*. (2001) proposed the following formulas

$$\frac{\phi P_e}{1.3P_y} \geq 1 \quad , \frac{P_e}{P_y} \geq 1.5 \quad (6)$$

Where $P_e$ is the buckling strength of the constrained element, $P_y$ is the yield strength of core elements and the strength reduction factor $\varphi$ of 0.85 was used in both equations.

An analysis of the elastic buckling of a composite brace composed of a steel core encased by a restrainer showed that the critical load of the entire brace member under compression could be found by solving an equilibrium equation as follows (Fujimoto *et al*. 1988)

$$E_b I_b . \frac{d^2 v}{dx^2} + (v + v_0) N_{max} = 0 \quad (7)$$

in which $E_B I_B$ is the flexural stiffness of the BRM, $N_y$ represents the brace yielding load, and $v$ and $v_0$ denote the transverse and the initial deflection of the brace member, respectively, as shown in Fig. 3. The initial deflection of the brace is assumed to be expressed by a sinusoidal curve as follows

$$v_0 = a \sin\frac{\pi x}{l} \quad (8)$$

where a is the initial deflection of the brace at the center, and $N$ is the brace axial load. Solving the equilibrium Eq. (7) results in the following

$$v + v_0 = \frac{a}{1-\dfrac{P_{max}}{P_c}} \sin\frac{\pi x}{l} \quad (9)$$

According to the paper referred by the reviwer and based on the study by Takeuchi *et al*. (2014) and Fujimoto *et al*. (1988) the bending moment at the center of BRM can be written as follows

$$M_y^B \geq \frac{(a+e+s_r)}{1-\dfrac{P_{cu}}{P_{cr}^R}} P_{cu} \quad (10)$$

where $P_{cu}$ is the maximum axial force of the brace. Assuming that $P_{cu}$ is equal to the $P_y$ (i.e., yield load of the core) and $M_y^B$ denotes yield bending strength of the restrainer, denotes maximum imperfection along the restrainer, $e$ denotes axial force eccentricity, $s_r$ denotes the core–restrainer clearance, $P_{cu}$ denotes the maximum axial strength of the core plates. $P_{cr}^R$ denotes the Euler buckling strength of the restrainer, This is the first formula that successfully expresses strength and stiffness require-ments as paired in the design of BRBs. Considering that the buckling of the BRB occurs when the maximum stress in the outermost fiber of the BRM reaches the yield stress, the requirement for stiffness and strength of the steel tube (BRM) can be obtained as follows

$$\frac{P_e}{P_y} \geq 1 + \frac{\pi^2 . E_B .(a+e+s_r).D}{2\sigma_y . L_B{}^2} \quad (11)$$

In which $L_B$, $\sigma_y$, and $D$ denote the length, the yield stress of the steel tube, and the depth of the restraining member section, respectively. In this formula, the effect of gap amplitude, $g$, has not been considered in the calculation of the moment at the center of the BRM. Therefore, in this paper, this parameter is involved in Eq. (10). Thus, Eq. (10) can be modified as follows

$$\frac{P_e}{P_y} \geq 1 + \frac{\pi^2 . E_B .(a+e+s_r+g).D}{2\sigma_y . L_B{}^2} = \beta \quad (12)$$

And based on the results obtained from the research

Table 1 Material and geometric properties of specimen 2 in ERYASAR's work (Eryasar 2009)

| Specimen | Core | | | Restraining member | | | | |
|---|---|---|---|---|---|---|---|---|
| | Dimension | Ratio | $F_y$ (MPa) | Section | Connection | Type of weld | Connection | Initial deflection |
| 2 | 40×5 | 8:1 | 355 | UPN65 | Weld | Continuous | Friction | No |

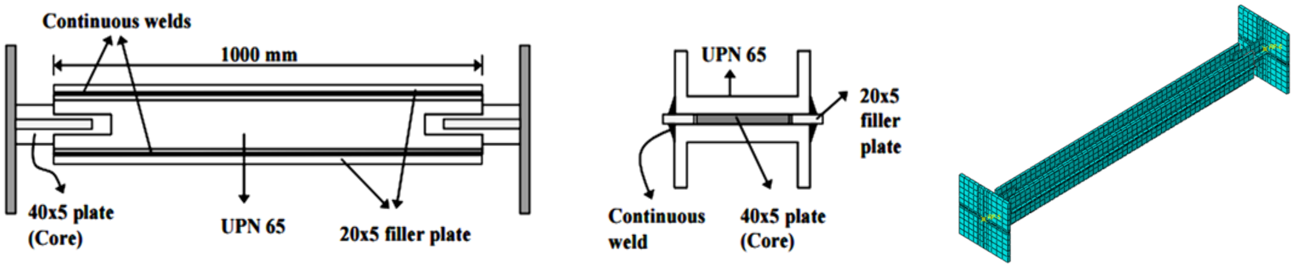


(a) Representative Drawing of Specimen 2 (Eryasar 2009) (b) Meshing of finite element model

Fig. 5 longitudinal , cross sectional and finite element view of specimen 2

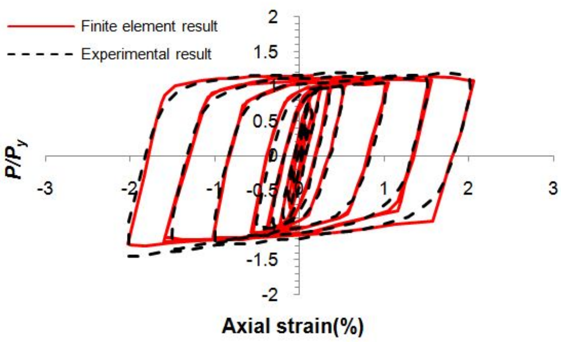


Fig. 6 Validation of finite element model with Eryasar laboratory results

conducted by Kato *et al*. (2002) at the moment of global buckling, the proposed formula mentioned above changes to

$$\frac{P_e}{P_y} \geq 1.03 + \frac{\pi^2.E_B.(a+e+s_r+g).D}{2\sigma_y.L_B^{\ 2}} = \beta \tag{13}$$

where $L_B$ is the length of the core and BRM (equal together), and D is the depth of the BRM section. Eq. (13) indicates that overall buckling of the brace will not occur if the ratio $P_e/P_y$ is greater than the parameter $\beta$, which is calculated based on the geometric characteristics and material characteristics of the brace member. This formula is for the case of BRBs with pin ends and without any firiction between core and BRM (models M1G0I0.5F0, M2G0I0F0, M3G0I0F0 and M4G0I0F0) as studied in this paper. In this paper, the overall buckling prevention condition of all-steel BRBs is numerically examined by the finite element analysis method. Among the 13 BRB models, two models (models M1G0I0.5F0 and M2G0I0F0) that had a $P_e/P_y$ ratio of less than 1.5 experienced global buckling during cyclic loading of the brace of up to a core strain of 2%. In those buckled BRBs, the $P_e/P_y$ ratios were less than factor $\beta$ in Eq. (13), which confirms the validity of that equation, whereas in the other two models(models without firiction between core and BRM), with a $P_e/P_y$ ratio greater than 1.5, no buckling was captured in the compression thus the result of this study confirms the validity of that equation for BRBs with pin ends and in the case of no friction between steel components and also confirms the proposed formulas by Chen *et al*. (2001).

Moreover, the other effective parameters in determination of bending moment include: the empty space between core and buckling restraining member, the initial deformation in bracing members and load eccentricity. The current research aims at investigating these braces behavior by removing concrete materials and converting it to all-steel braces, the numerical and software investigations of the behavior of these braces under cyclic loading will be conducted in finite element software, ABAQUS. Therefore, briefly the aims of this paper are:

(1) Investigating cyclic behavior of BRBs in finite element software, ABAQUS, after validation of modeling results.
(2) Investigating the effect of empty space parameter between core and restraining system.
(3) Investigating the effect of friction between core and restraining system on the global and local buckling behavior of the brace.
(4) Investigating the effect of the ratio of Euler buckling strength to core yield strength on the global buckling behavior of BRBs ($P_e/P_y$).

## 3. Comparison of finite element analysis results with laboratory results

In order to investigate the validity of results, at first, the finite element model was validated. For this purpose, one of he laboratory specimens which had been carried out by Eryasar (2009), was investigated and the results of finite element model were compared with the laboratory results. The cross section and the characteristics of laboratory specimen to be modeled in finite element software, ABAQUS, are shown in Table 1. During analysis, the axial displacement of core versus time is obtained and by dividing into the length of core, its axial strain is calculated. In addition, the axial force created at two ends under applied displacement is read and finally the load-displacement diagram resulted from finite element analysis and the results of performed tests for this brace were depicted in one diagram. As it is shown in Fig. 6, there is a good agreement between the results of finite element model and laboratory model and both models present a very stable cycle during loading. A finite element mesh representation of BRB members and Representative Drawing of Specimen 2 of ERYASAR's work are shown in Fig. 5.

Considering the good and close accordance of hysteresis responses of finite element analysis and laboratory results, it can be concluded that the finite element model was accurately modeled and with assumptions close to reality, and for more investigation, parametric study can be done on the effective parameters on response.

## 4. Parametric study

In order to better understand the cyclic behavior of of BRBs, a set of finite element analyses were performed on some BRBs specimens. In addition, to better portray the behavior of these braces, a three dimensional model of this brace was built in finite element software, ABAQUS. These models consist of the core, restraining member and filler plates.

### *4.1 Details and description of models*

A numerical study with various details was conducted on some BRBs specimens. Table 1 shows the specifications and descriptions of models. The first column of table is model name in which the M-index indicates the model's name and the number beside it, is the number relevant to that model. G-index indicates the empty space in vertical direction (gap), I-index is the initial deformation (imperfection), F-index indicates friction and the number beside it, is assumed to be the relevant analysis friction coefficient, in addition the schematic section of specimens is shown in Fig. 7.

As it can be seen in Table 1, in all specimens the core cross section is constant and equals 1000 mm$^2$ but the sections area of restraining system ($A_R$) and the second moment of interia of BRM ($I_R$) in models are different. Therefore, the yield stress of the core has been considered constant while the stiffness and resistance of restraining member differ. Moreover, the effect of providing a gap between core and buckling restraining members has been mentioned in analysis. In parametric study, the total length of BRBs has been considered to be 2000 mm. The yield load of steel plate, $P_y$, has been obtained by multiplying the plate yield stress and its cross-sectional area. The buckling load of restraining members (BRM), $P_e$ also has been obtained using Euler buckling load equation.

Steel core and the other members of brace were modeled by C3D8R elements with eight nodes. A static analysis of finite element was carried out on the specimens by the use of ABAQUS software. Moreover the full Newton-Raphson method was used to solve the nonlinear equations during analysis. In addition, to simplify the convergence, automatic stabilization with damping coefficient of 0.0002 was considered. A nonlinear static problem can be unstable, this instability may be due to natural geometry, the nature of materials such as materials hardening or buckling. ABAQUS software provides an automatic mechanism for consolidation and stabilization of quasi-static unstable problems by adding damping proportional to volume (Abaqus 2010).

As it is expected that the core experiences large plastic deformations and higher buckling modes, a fine meshing was considered for core in cross section with two elements in thickness and 5 elements or more in width. For buckling restraining members, meshing with coarser elements was considered and it is expected that these elements remain elastic.

In this study the interface between steel components is modeled using the surface-to-surface contact elements with an approximate automatic stabilization factor of 1E-4 to achieve a better convergence. To simulate a greasy smooth interface between core and restraining member, in the form

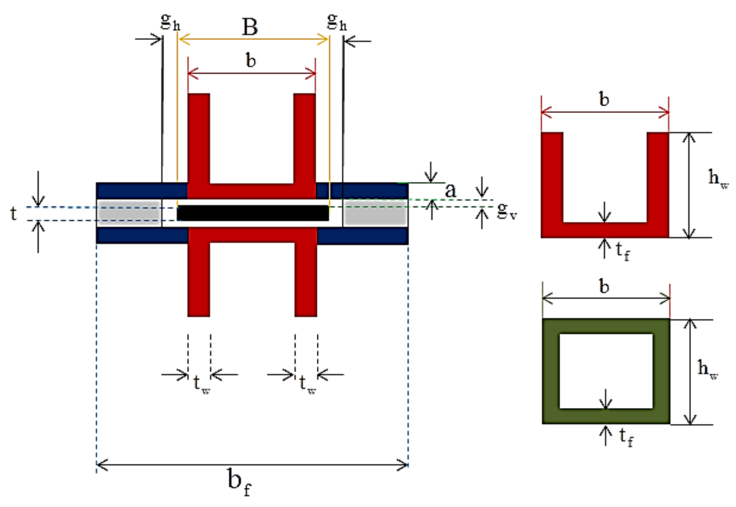


Fig. 7 The section of BRB modeled in ABAQUS software

Table 2 The geometric properties of specimens modeled in ABAQUS software

| Model | $a$ | $b_f$ | $t_f$ | $b$ | $t_w$ | $g_v$ | $g_h$ | $I_R$ | $A_R$ | $P_e/P_y$ | $\beta$ | Local buckling | Global buckling |
|---|---|---|---|---|---|---|---|---|---|---|---|---|---|
| M1G0I0. 5F0 | 5 | 140 | 5 | 50 | 7 | 0 | 1 | 817566 | 2704 | 1. 1 | 1.15 | No | Yes |
| M2G0I2F0 | 6 | 140 | 5. 5 | 65 | 6 | 0 | 1 | 977849 | 3015 | 1. 3 | 1.28 | No | Yes |
| M3G0I2F0 | 8 | 140 | 5 | 80 | 6 | 0 | 1 | 1124713 | 3100 | 1. 5 | 1.42 | No | No |
| M4G0I2F0 | 6 | 140 | 4 | 42 | 4 | 0 | 1 | 1199868 | 2772 | 1. 6 | 1.37 | No | No |
| M3G0I2F0. 05 | 8 | 140 | 5 | 80 | 6 | 0 | 1 | 1124713 | 3100 | 1. 5 | | No | Yes |
| M4G0I2F0. 05 | 6 | 140 | 4 | 42 | 4 | 0 | 1 | 1199868 | 2772 | 1. 6 | | No | Yes |
| M3G1I2F0. 05 | 8 | 140 | 5 | 80 | 6 | 1 | 1 | 1216619 | 3176 | 1. 62 | | Yes | No |
| M4G1I2F0. 05 | 6 | 140 | 4 | 42 | 4 | 1 | 1 | 1286613 | 2848 | 1. 72 | | Yes | No |
| M4G0I2F0. 1 | 6 | 140 | 4 | 42 | 4 | 0 | 1 | 1199868 | 2772 | 1. 6 | | Yes | Yes |
| M3G1I2F0. 1 | 8 | 140 | 5 | 80 | 6 | 1 | 1 | 1216619 | 3176 | 1. 62 | | Yes | Yes |
| M4G1I2F0. 1 | 6 | 140 | 4 | 42 | 4 | 1 | 1 | 1286613 | 2848 | 1. 72 | | Yes | No |
| M3G2I2F0. 1 | 8 | 140 | 5 | 80 | 6 | 2 | 1 | 1314876 | 3252 | 1. 75 | | Yes | No |
| M5G0I2F0. 1 | 5 | 140 | 3 | 50 | 3 | 0 | 1 | 1487851 | 2408 | 1. 98 | | No | No |

of tangential Coulomb frictional behaviors, a general contact between members was defined in which various values (0, 0.05 and 0.1) were assumed for friction coefficient. The same frictional coefficient was considered in the similar analysis conducted by Chou and Chen (2010). Actually, the value of friction coefficient has a very significant effect on the buckling behavior of these braces. That is why; one of the studied parameters in this study is the effect of friction coefficient on the buckling behavior of these braces. The larger the friction coefficient, the more the forces are transferred from core to BRM system in compressive loading which is due to more contact of core and restraining members. This causes the BRM system to become closer to Euler buckling load. Therefore, the global buckling behavior of BRBs is affected by the change of friction coefficient value. A hard contact rule was assumed to minimize the penetration of steel surfaces too. The contact model allowed for the separation of the core plate from the BRM elements, which enabled higher mode buckling of the core plate.

In this paper to simulate geometry imperfections an initial deformation of 2 mm was considered both at the core and at restraining member for all specimens, also boundary conditions are shown in Fig. 9. Therefore, a predefined

Table 3 Steel material properties assumed in parametric study

| Poisson ratio | $F_y$ (MPa) | Young modulus |
|---|---|---|
| 0.3 | 370 | 200 GPa |

linear static analysis was carried out to apply an initial small deformation to model before beginning a nonlinear cyclic analysis. For this reason, a widespread parabolic load (in which it is zero at both ends and at the center it is maximum) was considered at the initial stage on the core and BRM system so that deformation at the middle of the brace reaches to desirable value of 2 mm. After this stage, axial compression loading is applied to core section at both ends.

Considering the gap between the core and BRM system, the analysis of finite elements can be divided into 3 groups, that in the first group the core and BRM are in direct contact to each other. In the second group, the gap between the core and BRM from top and down (along the thickness) is 1 mm; and in the third group it was considered to be 2 mm. In addition, a gap of 1 mm was considered between core and BRM along the core width. The rotation of brace is free around the main axes while the rotation around the longitudinal axis has been restrained.

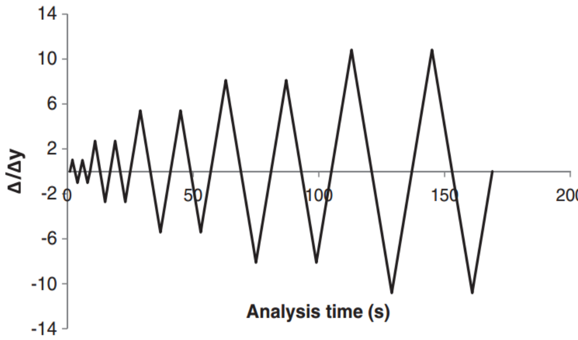


$U_x = U_y = UR_z = UR_y = 0$

Fig. 8 The loading protocol used in analysis

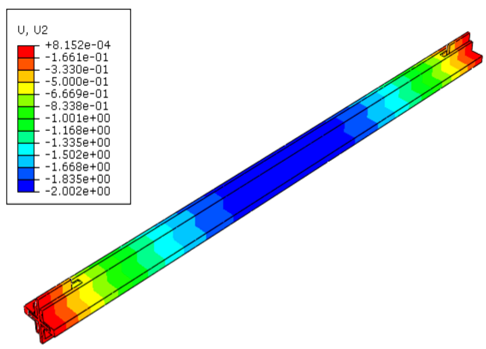


$U_x = U_y = UR_z = UR_y = 0$

Fig. 9 Applying initial deflection

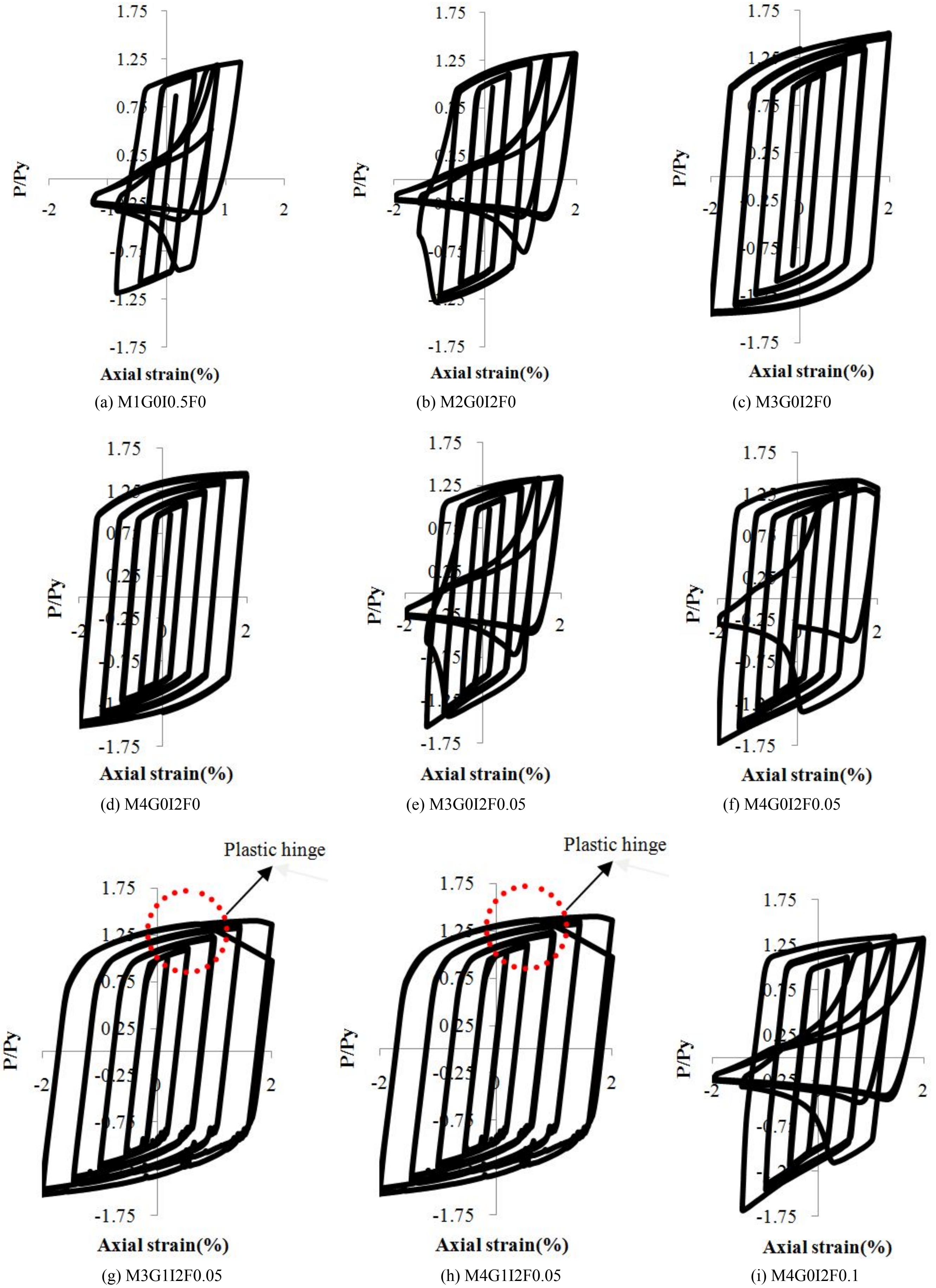


(a) M1G0I0.5F0 (b) M2G0I2F0 (c) M3G0I2F0

(d) M4G0I2F0 (e) M3G0I2F0.05 (f) M4G0I2F0.05

(g) M3G1I2F0.05 (h) M4G1I2F0.05 (i) M4G0I2F0.1

Fig. 10 Hysteresis responses of BRBs

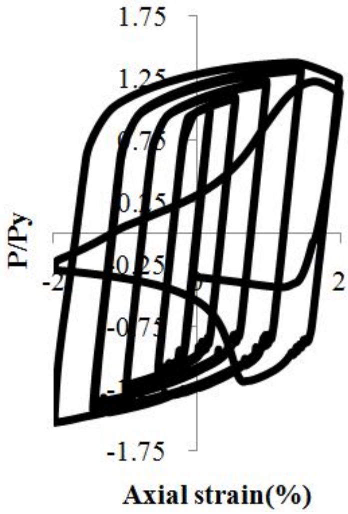

(j) M3G1I2F0.1

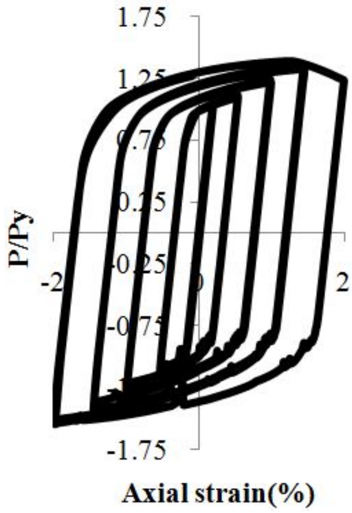

(k) M4G1I2F0.1

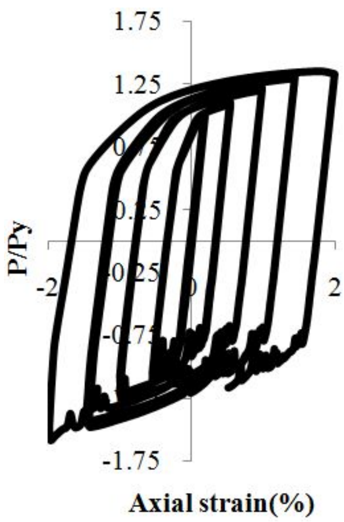

(l) M3G2I2F0.1

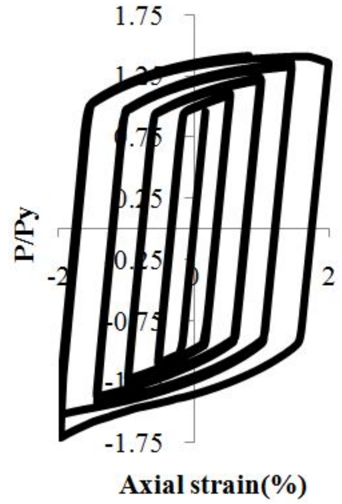

(m) M5G0I2F0.1

Fig. 10 Continued

The assumptions in the parametric study for core plate and the BRM and other steel components material properties are given in Table 3.

The hardening behavior rule of most materials appears to be a combination of the isotropic and kinematic type of hardening, sometimes accompanied by a change of shape of the yield surface. A nonlinear combined isotropic-kinematic hardening rule has been performed for different material properties in order to properly simulate real materials. The selection and calibration hardening parameters of steel material were based on Coupon and cyclic test results conducted by Tremblay *et al*. (2006) and further analytical studies by Korzekwa and Tremblay (2009). Based on those studies, the initial kinematic hardening modulus C and the rate factor $\gamma$ were set to 8 GPa and 75, respectively (Korzekwa and Tremblay 2009). For isotropic hardening, a maximum change in yield stress of $Q_\infty$ = 110 Pa and a rate factor of $b$ = 4 were adopted. A nonlinear static problem can be unstable. Such instabilities may be of a geometrical nature, such as buckling, or of a material nature, such as material softening. ABAQUS provides an automatic mechanism for stabilizing unstable quasi-static problems through the automatic addition of volume-proportional damping to the model. The adaptive automatic stabilization scheme, in which the damping factor can vary spatially and with time, provides an effective alternative approach. In this case the damping factor is controlled by the convergence history and the ratio of the energy dissipated by viscous damping to the total strain energy. If the convergence behavior is problematic because of instabilities or rigid body modes, ABAQUS automatically increases the damping factor (Hoveidae and Rafezi 2012). In this study, the default accuracy tolerance of 0.04 was assumed for adaptive stabilization. Also, maximum and minimum increment sizes of 0.2 and 1E-8, respectively, were specified in the analysis. Based on the cyclic quasi static protocol suggested by AISC seismic provisions for BRBs (2010) axial displacements were applied at both end as follows: 2 cycles at $\pm\Delta_y$, 2 cycles at $\pm 0.5\Delta_{bm}$, 2 cycles at $\pm\Delta_{bm}$, 2 cycles at $\pm 1.5\Delta_{bm}$, and 2 cycles at $\pm 2\Delta_{bm}$, where $\Delta_y$ is the yield displacement of the core, and $\Delta_{\mathrm{bm}}$ is the axial deformation of the brace corresponding to the design story drift (Tremblay *et al*. 2006). According to previous studies by Tremblay *et al*. (2006), the range peak strain amplitude in full-length core braces is 0.01 to 0.02, and this peak deformation range was used in many previous test programs (Watanabe *et al*. 1988). Thus Considering the axial strain of 1% in the core, in this study $\Delta_{bm}$ = 20 mm, and the core $\Delta_y$ = 3.7 mm based on the material characteristics. Fig. 8 shows the loading protocol used in the analyses.

## 5. Discussions of results

Hysteresis responses of BRBs have been predicted very well by finite element models whether in linear range or nonlinear range. Figs. 10(a)-(m) shows the hysteresis responses of braces in which the horizontal axis of displacement is along the longitudinal direction of brace and the vertical axis of axial force is imposed on the end of the brace. These diagrams represent accurately the reduction in resistance resulted from the global or local buckling in braces.

The relation of the axial loading ($P/P_y$) and axial strain of each analysis shown in Fig. 10 demonstrate the sudden decline in strength and global buckling in compression cycles in the models M1G0I0.5F0, M2G0I2F0, M3G0I2F0.05, M3G0I2F0.05, M4G0I2F0.05, M4G0I2F0.1 and M3G1I2F0.1 while in the other models, hysteretic response with approximately identical behavior in tension and compression sides without any perceptible change in the force-deformation curves is specified. The sudden decline in strength in tension cycles in the models M3G1I2F0.05 and M4G1I2F0.05 is due to forming plastic hinge in the middle of core plate at the end of loading as can be seen in Fig. 12(f). As it is obvious from Table 2, in no friction case for ratios higher than $P_e/P_y \geq 1.5$, global buckling up to strain of 2% does not happen during axial loading. But as in reality there is friction between different members, the value of this parameter increased in next stages to investigate its effect on the global buckling behavior. Therefore, at the next stage this value increased up to 0.05. As it is evident, in model M3G0I2F0 (Fig. 10(c)) which has shown a very stable behavior in frictionless condition, by adding this coefficient in the software, the global buckling has occurred in brace (Fig. 10(e)). This phenomenon observed for model M4G0I2F0.05 as well, with this difference that in this model, the global buckling phenomenon has occurred at the last cycle due to larger ratio of $P_e/P_y$. Actually, the increase of this ratio helps with postponing the total buckling phenomenon. In this case, in order to prevent buckling phenomenon in the presence,

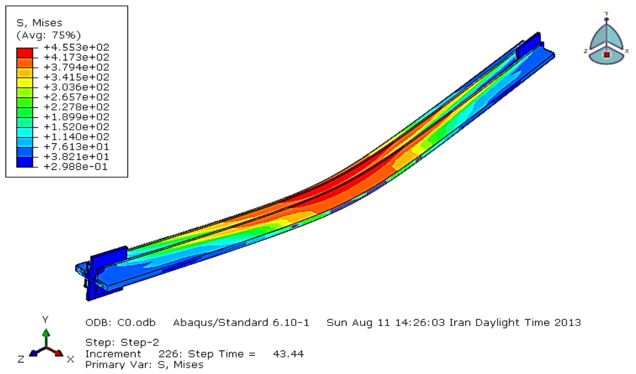


Fig. 11 Global buckling of model M1G0I0.5F0

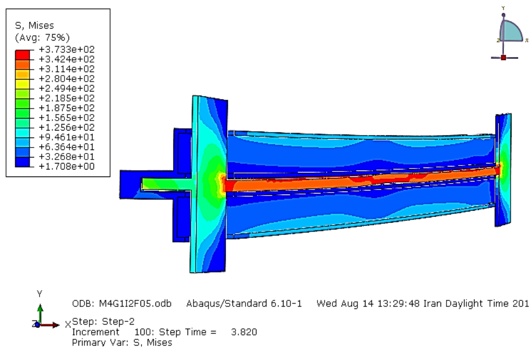


(a) Deflection of model M4G1I2F0.05 at $\Delta/\Delta_y$ = 0.1

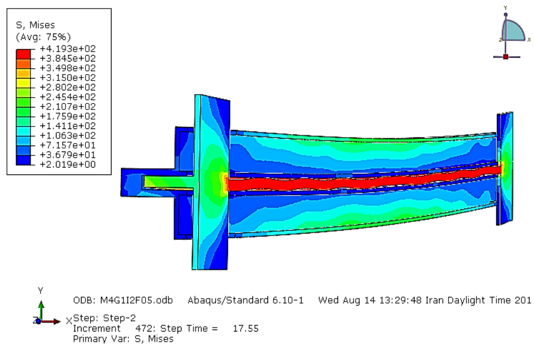


(b) Deflection of model M4G1I2F0.05 at $\Delta/\Delta_y$ = 0.27

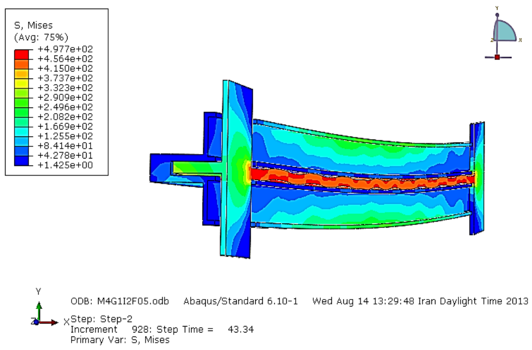


(c) Deflection of model M4G1I2F0.05 at $\Delta/\Delta_y$ = 0.5

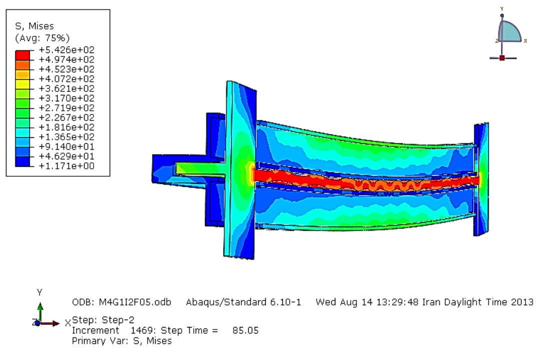


(d) Deflection of model M4G1I2F0.05 at $\Delta/\Delta_y$ = 0.73

Fig. 12 Deflection and Formation of plastic hinge of model M4G1I2F0.05 up to end of loading

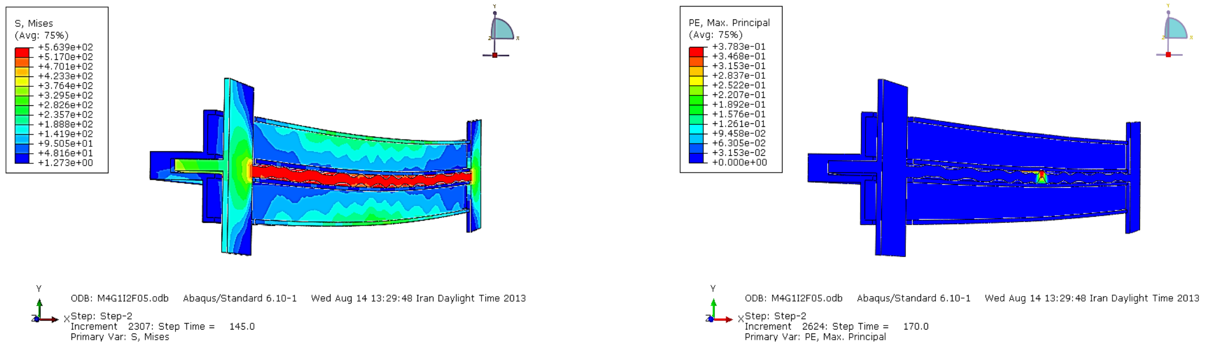


(e) Deflection of model M4G1I2F0.05 at $\Delta/\Delta_y = 1$

(f) Formation of plastic hinge in the middle of core

Fig. 12 Continued

a gap was provided between core and BRM system that let the core buckle in higher modes and shows a more stable behavior. Therefore, as it was expected by providing a gap of 1 mm in each side between core and BRM, the global buckling phenomenon was not seen during loading cycles in model M3G1I2F0.05 (Fig. 10(g)). Also, due to providing a gap between core and BRM, a little reduction in strength is seen in some points. The cause of this phenomenon occurrence is that the core experienced local buckling in these points and then it reached balance and the global buckling did not occur.

At last stage, the value of friction coefficient increased to 0.1. In this case, like the previous model (model M4G0I2F0.05 with the friction coefficient of 0.05) in which global buckling was not seen, by increasing friction coefficient to 0.1 the global buckling phenomenon occurred (Fig. 10(i)). Therefore, it can be concluded that friction has an important role in response and will affect the global buckling significantly. In model M3G2I2F0.1 with friction coefficient of 0.1 (Fig. 10(l)), the gap between core and BRM reached to 2 mm and it was seen that by increasing distance, the amount of local buckling increases and greater changes were seen in the BRBs response in comparison with the case of 1 mm distance, but finally brace shows stable response to the exerted displacement and global buckling will not happen in ratio of $P_e/P_y$ equal to 1.75. In model M5G0I2F0.1 in which the ratio of $P_e/P_y$ equals 1.98, in spite of friction coefficient of 0.1, the global buckling was not seen in it (Fig. 10(m)).Fig. 11 shows the buckled shape of model M1G0I0.5F0 including the von misses stress contours.

The deflection of the BRM during compression cycles ascribable to higher order buckling of the core in model M4G1I2F0.05 is shown in Figs. 12(a)-(e). As it can be seen, outward forces imposed due to local buckling from the core member to BRM are resisted by upper and lower BRM components so that the BRM remains elastic because of its large rigidity. Also the number of local buckles at large compression loads is more closely spaced at the middle of core.

According to the above results, the suggestion for a global buckling prevention condition of all-steel BRBs is $P_e/P_y \geq 1.5$ in the case of there is no friction between the core and BRM members which is completely coincident with the equation suggested by Chen *et al*. (2001). But this

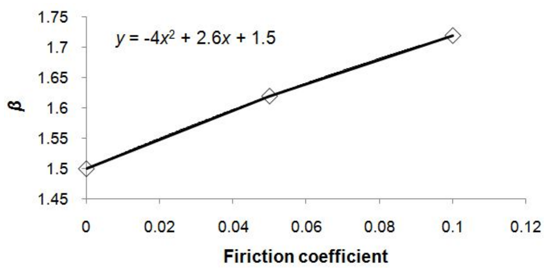


Fig. 13 The relation between $\beta$ and friction

ratio increases for mentioned condition in the presence of friction between steel components.

Thus according to the result of this study and considering the relation between various friction coefficient and factor $\beta$ shown in Fig. 13, the proposed equation involving friction coefficient can be

$$\frac{P_e}{P_y} \geq \beta + 2.4(F) \tag{14}$$

Where $F$ is the friction coefficient between core and BRM in BRBs with pin ends.

## 6. Conclusions

One of the main required performances of BRBs is to prevent bracing member from experiencing global buckling until it reaches enough plastic deformation and required ductility. The new generation of BBRs which are called steel buckling restrained braces, are a group of unbuckling braces with lighter members in comparison to conventional unbuckling braces. In this group of unbuckling braces, a light steel member is used as a restraining member against buckling instead of common concrete-filled sections, which may lead to global buckling of the brace due to insufficient stiffness and lack of required resistance restraining members.

In this paper, these types of braces behavior and the conditions to prevent global buckling in them were studied and investigated using a set of finite element analysis through using ABAQUS software.

Different models with various proportions of $P_e/P_y$

under cyclic loading and the response of load to the imposed displacement was depicted in a diagram. Moreover, in these diagrams the friction coefficient was one of the studied parameters during analysis in these specimens. The hysteresis response of specimens showed that based on the results of this study, when the effect of friction, for a brace not to have global buckling, the ratio of $P_e/P_y$ should not be less than 1.5 to avoid global buckling of the brace. By increasing the friction coefficient of contact between the core and BRM system, the frictional response increases and the buckling behavior of brace will be affected. When the magnitude of the coefficient of friction between the core and the buckling restraining member is high, the slip of the core under compressive loading within its covering members will not take place easily and finally, result in very great shear force and the lateral bending of the brace under compressive force. In addition, the formed shear forces in the inner surface will result in the increase of transitive axial force to BRM system with initial deformation which may lead to the bending buckling of the brace. Therefore, as shown in Table 2, according to the conducted analyses in this research, by increasing friction coefficient, according to conducted analysis the ratio of $P_e/P_y$ should not be less than 1.62 in order to avoid global buckling of the brace. Another parameter that was studied in this paper was providing a gap between core and BRM system; this gap was considered to be 1 mm and 2 mm in different specimens. The hysteresis response of specimens showed that by providing this gap, even in spite of some local instabilities related to higher buckling modes in the core, the hysteresis response of brace will not be affected significantly unless the stiffness and strength of restraining members are sufficient. So, the existence of this gap will help that core buckles in higher modes and shows a more stable behavior. Following that, the friction coefficient reached to 0.1 and it was observed that again by increasing this coefficient, the global buckling behavior of the brace will be influenced, and in this case the ratio of $P_e/P_y$ should not be less than 1.7 based on the results.

## References

Abaqus (2010), Abaqus analysis user's manual; Version 6.10, Dassault Systems.

AISC (American Institute of Steel Construction) (2010), Seismic provisions for structural steel buildings, Chicago, IL, USA.

ATC-40 (1996), Seismic evaluation and retrofit of concrete buildings, Redwood City, CA, USA.

Black, C.J., Makris, N. and Aiken, I.D. (2002), "Component testing, stability analysis, and characterization of buckling restrained braced braces", PEER Report No. 2002/08; University of California, CA, USA.

Chen, C.C., Chen, S.Y. and Liaw, J.J. (2001), "Application of low yield strength steel on controlled plastification ductile concentrically braced frames", *Can. J. Civil Eng.*, **28**(5), 823-836.

Chen, Q., Wang, C.L., Meng, S. and Zeng, B. (2016), "Effect of the unbonding materials on the mechanic behavior of all-steel buckling-restrained braces", *Eng. Struct.*, **111**(15), 478-493.

Chou, C. and Chen, S. (2010), "Sub-assemblage tests and finite element analyses of sandwiched buckling restrained braces", *Eng. Struct.*, **32**(8), 2108-2121.

Eryasar, M.E. (2009), "Experimental and numerical investigation of buckling restrained braces", M.S. Thesis; Middle East Technical University, Ankara, Turkey.

Fahnestock, L.A., Sause, R. and Ricles, J.M. (2007), "Seismic response and performance of buckling-restrained braced frames", *J. Struct. Eng.*, **133**(9), 1195-1204.

Fujimoto, M., Wada, A., Saeki, E., Watanabe, A. and Hitomi, Y. (1988), "A study on the unbonded brace encased in buckling restraining concrete and steel tube", *J. Struct. Construct. Eng.*, **34B**, 249-258.

Hoveidae, N. and Rafezy, B. (2012), "Overall buckling behavior of all-steel buckling restrained braces", *J. Construct. Steel Res.*, **79**, 151-158.

Jiang, Z., Guo, Y., Zhang, B. and Zhang, X. (2015), "Influence of design parameters of buckling-restrained brace on its performance", *J. Construct. Steel Res.*, **105**, 139-150.

JSSC (1998), Seismic Responses and Seismic Design Methods of Frames with Hysteretic Dampers, Tokyo, Japan.

Kato, M., Usami, T. and Kasai, A. (2002), "A numerical study on cyclic elasto-plastic behavior of buckling-restraining brace members", *Struct. Eng. Earthq. Eng.*, **48A**, 641-648.

Kim, J. and Choi, H. (2004), "Behavior and design of structures with buckling-restrained braces", *Eng. Struct.*, **26**(6), 693-706.

Kim, S.H. and Choi, S.M. (2015), "Structural behavior of inverted V-braced frames reinforced with non-welded buckling restrained braces", *Steel Compos. Struct., Int. J.*, **19**(6), 1581-1598.

Korzekwa, A. and Tremblay, R. (2009), *Behaviour of Steel Structures in Seismic Areas*, CRC Press, Montreal, QC, Canada.

Mazzolani, F. and Tremblay, R. (2000), *Behaviour of Steel Structures in Seismic Areas: STESSA 2000*, A.A. Balkema, Montreal, QC, Canada.

Pandikkadavath, M.S. and Sahoo, D.R. (2016), "Cyclic testing of short-length buckling-restrained braces with detachable casings", *Eartq. Struct., Int. J.*, **10**(3), 699-716.

Park, J., Lee, J. and Kim, J. (2012), "Cyclic test of buckling restrained braces composed of square steel rods and steel tube", *Steel Compos. Struct., Int. J.*, **13**(5), 423-436.

Sabelli, R., Mahin, S. and Chang, C. (2003), "Seismic demands on steel braced frame buildings with buckling-restrained braces", *Eng. Struct.*, **25**(5), 655-666.

Takeuchi, T., Hajjar, J.F., Matsui, R., Nishimoto, K. and Aiken, I.D. (2012), "Effect of local buckling core plate restraint in buckling restrained braces", *Eng. Struct.*, **44**, 304-311.

Takeuchi, T., Ozaki, H., Matsui, R. and Sutcu, F. (2014), "Out-of-plane stability of buckling-restrained braces including moment transfer capacity", *Earthq. Eng. Struct. Dyn.*, **43**(6), 851-869.

Talebi, E., Tahir, M.M., Zahmatkesh, F. and Kueh, A.B. (2015), "A numerical analysis on the performance of buckling restrained braces at fire-study of the gap filler effect", *Steel Compos. Struct., Int. J.*, **19**(3), 661-678.

Tremblay, R., Bolduc, P., Neville, R. and DeVall, R. (2006), "Seismic testing and performance of buckling restrained bracing systems", *Can. J. Civil Eng.*, **33**(2), 183-198.

Usami, T., Ge, H. and Luo, X. (2009), "Experimental and analytical study on high-performance buckling restrained brace dampers for bridge engineering", *Proceeding of 3rd International Conference on Advances in Experimental Structural Engineering*, San Francisco, CA, USA, October.

Watanabe, A., Hitomi, Y., Yaeki, E., Wada, A. and Fujimoto, M. (1988), "Properties of braces encased in buckling-restraining concrete and steel tube", *Proceedings of 9th World Conference on Earthquake Engineering*, Tokyo-Kyoto, Japan, August.

Wu, B. and Mei, Y. (2015), "Buckling mechanism of steel core of buckling-restrained braces", *J. Construct. Steel Res.*, **107**, 61-69.

Zhao, J., Wu, B., Li, W. and Ou, J. (2014), "Local buckling behavior of steel angle core members in buckling-restrained braces: Cyclic tests, theoretical analysis, and design recommendations", *Eng*. *Struct*., **66**, 129-145.

*CC*